



Nano-Communications: A New Field? An Exploration into a Carbon Nanotube Communication Network

Stephen F. Bush and Yun Li

2006GRC066, February 2006

Public (Class 1)

Technical Information Series

Copyright © 2006. Inderscience Publishers. Used with permission.

GE Global Research

Technical Report Abstract Page

Title Nano-Communications: A New Field? An Exploration into a Carbon Nanotube Communication Network

Author(s) Stephen F. Bush **Phone:** 8*833-6827
Yun Li

Component Report Advanced Communication Systems Laboratory, Niskayuna

Number 2006GRC066 **Date** February 2006

Number of Pages 26 **Class** Public (Class 1)

Key Words: Carbon nanotube network, communication network, nano-scale sensor network, embedded communication network, molecular information routing

Abstract: Imagine a communication network constructed at a nanometer scale. This paper examines the potential benefits from the perspective of using individual nanotubes within random carbon nanotube networks (CNT) to carry information. This is distinct from traditional, potentially less efficient, approaches of using CNT networks to construct transistors. The traditional networking protocol stack is inverted in this approach because, rather than the network layer being logically positioned above the physical and link layers, the CNT network and routing of information is an integral part of the physical layer. Single-walled carbon nanotubes (SWNT) are modelled as linear tubes positioned in two dimensions via central coordinates with a specified angle. A distribution of lengths and angles may be specified. A network graph is extracted from the layout of the tubes and the unprecedented ability to route information close to the level of individual nanotubes is considered. The impact of random tube characteristics, such as location and angle, upon the corresponding network graph and its impacts are examined.

Manuscript received January 30, 2006

Nano-Communications: A New Field? An Exploration into a Carbon Nanotube Communication Network

Stephen F. Bush¹ and Yun Li²

¹*CDS, GE Global Research, Niskayuna, NY, 12309, USA*

²*MNST, GE Global Research, Niskayuna, NY, 12309, USA*

Email Address: bushsf@research.ge.com and liyun@research.ge.com

Imagine a communication network constructed at a nanometer scale. This paper examines the potential benefits from the perspective of using individual nanotubes within random carbon nanotube networks (CNT) to carry information. This is distinct from traditional, potentially less efficient, approaches of using CNT networks to construct transistors. The traditional networking protocol stack is inverted in this approach because, rather than the network layer being logically positioned above the physical and link layers, the CNT network and routing of information is an integral part of the physical layer. Single-walled carbon nanotubes (SWNT) are modelled as linear tubes positioned in two dimensions via central coordinates with a specified angle. A distribution of lengths and angles may be specified. A network graph is extracted from the layout of the tubes and the unprecedented ability to route information close to the level of individual nanotubes is considered. The impact of random tube characteristics, such as location and angle, upon the corresponding network graph and its impacts are examined.

A CNT network is rich in nanotubes. Many tubes, often in random orientations, can be densely packed. Current technology is focused on utilizing an entire CNT network as semiconducting material to construct a single transistor or Field Effect Transistor (FET).

Many such transistors are required to build legacy network equipment. The result is that there are many nano-scale networks embedded within each device that might be otherwise more effectively utilized for communication. Consider re-thinking the communication architecture such that the CNT network itself is the communication media and individual nanotubes are the links. Individual tubes and tube junctions (forming nodes) do not have the equivalent processing capability of a traditional network link and network node, thus it is important to consider methods to compensate for this by leveraging large numbers of tubes. An abstract comparison of communication and SWNT networks is shown in Figure 1. At the bottom level, communication links may be between hosts and routers in a communication network or they may be carbon nanotubes overlapping at points that will be identified as nodes. A network functions by changing state; data must either flow or be switched or routed through nodes. State may be implemented as a routing table on a router or an electromagnetic field controlling the resistance within a specific area of a carbon nanotube network. Finally, a mechanism needs to be in place to control state, be it a routing algorithm or FET gate voltages applied to a carbon nanotube network. The remainder of this paper discusses some of the properties of CNT networks relevant to communications such as bandwidth, capacity, and the impact of tube alignment. Then addressing and routing are discussed.

Basic Network Components	Traditional Networking	Nano-scale Networking
Protocol	Processors	Gate Control
State	Node Memory	Semiconducting Tube Resistance
Network	Links	Nanotubes

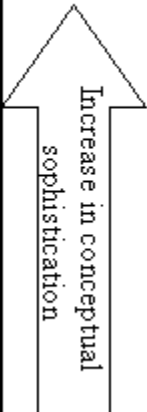


Figure 1 Network components for nano-scale networking requires modification of networking concepts to best fit the nano-scale environment.

The impact of scale on a traditional communication network is considered as the network is scaled down to the size of a carbon nanotube network. An obvious consideration from a network perspective is the change in capacity, specifically in bandwidth. Simple harmonic oscillation, which provides bandwidth, increases with reduction in scale; thus potential bandwidth increases dramatically. The increase is $1/L$ where L is a linear scale dimension. The capacity, C_{ij} , of a link from a transmitter at j to a receiver at i is given by Shannon's famous formula (1). Considering all possible multi-level and multi-phase encoding techniques, the theorem states that the theoretical maximum rate of clean (or arbitrarily low bit error rate) data with a given average signal power that can be sent through an analog communication channel subject to additive, white, Gaussian-distribution noise interference is:

$$C_{ij} = BW \ln(1 + (S/N)_{ij}) \quad (1)$$

The term BW is the bandwidth of the communication and $(S/N)_{ij}$ is the signal-to-noise ratio (SNR) of the link. SNR measures the ratio between noise and an arbitrary signal on the channel, not necessarily the most powerful signal possible. In Figure 2 the channel capacity, assuming noise is minimal (SNR=1/2), rises as the scale is reduced towards zero using (1).

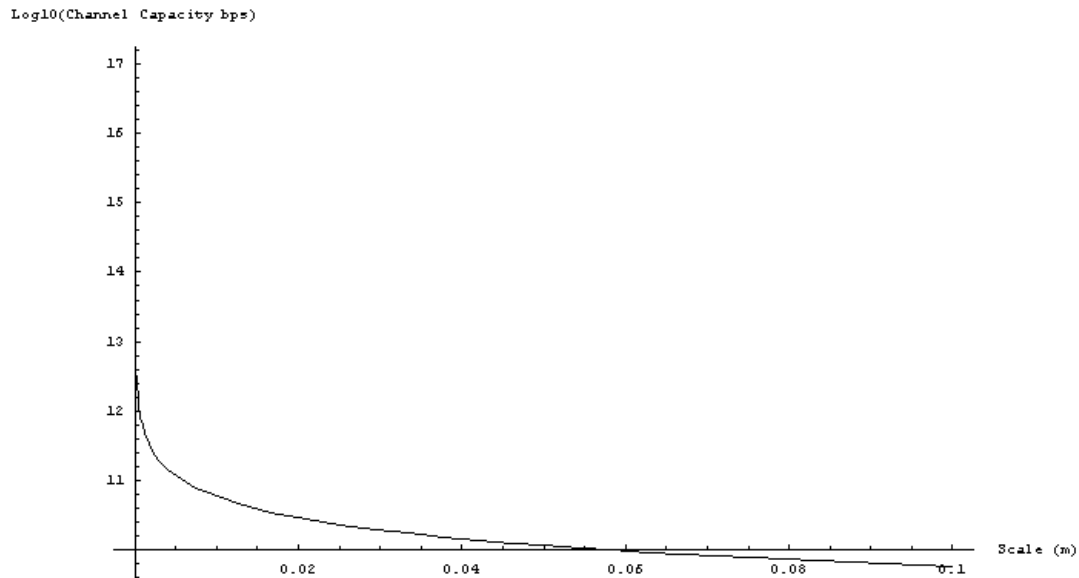


Figure 2 The approximate capacity increase with reduced scale is shown. As the scale becomes smaller, the potential capacity grows significantly.

In addition to the increased bandwidth potential, the nanotube density allows for an increase in the number of bits per square meter. Consider a wireless network of today. A typical bit-meters/second capacity is limited in a traditional wireless network as described in Ref. 3. The maximum wireless capacity approximation Ref. 3 in a wireless broadcast media can be used to determine the collective capacity. Now that the minimum amount of information to be propagated has been determined, it must be propagated throughout the network as efficiently as possible. In this case, assume a perfect

distribution mechanism in which all links are used as efficiently as possible to disseminate route update information. Assume a network of n nodes is spread over an area A and each possible connection has capacity W . Also, assume Δ is a guard distance to ensure channel transmissions do not overlap. The maximum wireless capacity in bit-meters per second is shown in (2).

$$C_{\max} = \sqrt{\frac{8}{\pi}} \frac{W}{\Delta} \sqrt{n} \quad (2)$$

Generalizing to a uniformly random distribution of n sensors over a circular area A , the density is $\frac{n}{A}$, and the expected nearest-neighbour distance is $\frac{\sqrt{A}}{n}$. The total distance that data must travel is shown in (3).

$$E[d] = \sum_{k=1}^n \frac{\sqrt{A}}{n} \quad (3)$$

Now consider a carbon nanotube network. A point source could radiate information omni-directionally via a tube structure limited by the degree of compactness of the tube network. If tubes could be well aligned, then the notion of a guard distance would be unnecessary. A macroscopic source is assumed to generate data omni directionally. A carbon nanotube is on the order of 1.4 nm in diameter. If tubes radiate compactly from a circular source, the capacity is shown in Figure 3. Essentially, the limit is reached as an extremely large number of tubes are joined to the source without overlapping. Unfortunately, current technology cannot align tubes with this degree of accuracy.

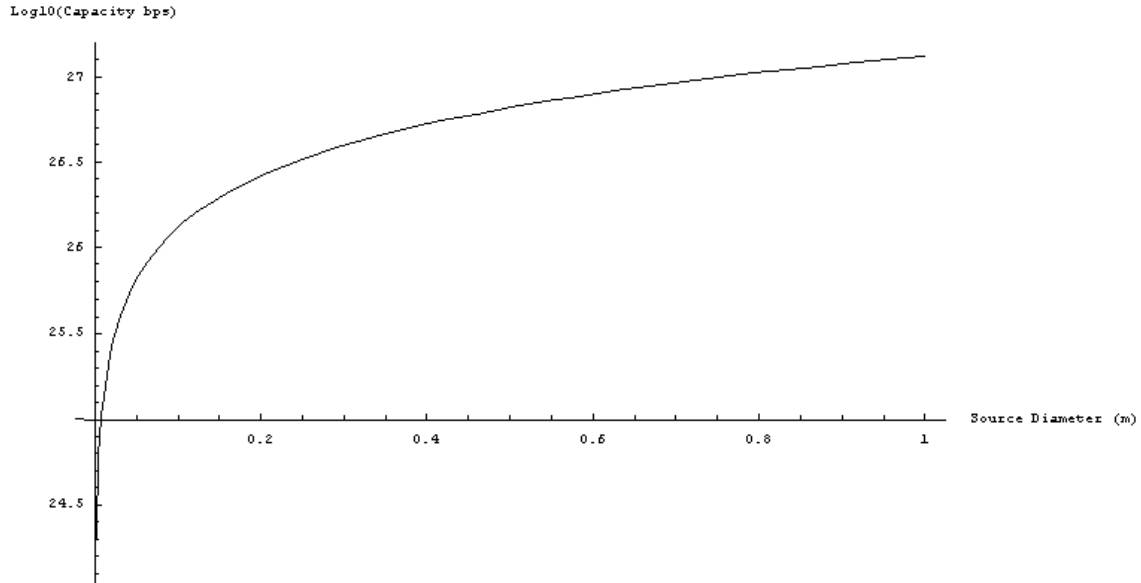


Figure 3 The capacity of a carbon nanotube network is shown as a function of the area available for nanotube connectivity. This is significantly higher capacity over much smaller distances than could be achieved with a wireless network.

A Mathematica¹ framework for evaluating random CNT networks has been developed and is being used to verify design characteristics of carbon nanotubes. The framework relates tube placement characteristics comprised of tube center location t_{xy} , tube angle θ , and tube density d_t . The intersections of tubes form vertices V and tubes form edges E of a graph $G(V, E)$. In the specific instance of FET mobility, the graph structure impacts the mobility μ of the FET. Thus, a goal has been to find the relationship among tubes, the CNT network, and mobility¹. Let $f(t_{xy}, \theta, d_t)$ be a function of physical tube characteristics. Mobility is approximated as $\frac{L_{sd}(I_{on}-I_{off})}{w} \frac{t_{ox}}{20\epsilon V_{sd}}$ where I_{on}

¹ A Mathematica package has been developed that constructs a CNT network from a tube layout and has supported the analytical development of CNT network properties.

and I_{off} are FET gate ‘on’ and ‘off’ currents that are determined by the resistance of a CNT network; w and L_{sd} are the gate width and length respectively.

$$f(t_{xy}, \theta, d_t) \longrightarrow G(V, E) \longrightarrow \mu(\Delta R_{sd}) \quad (4)$$

A key component of the tube layout is the overall directionality of the tubes, that is, the angle of each tube relative to all other tubes. Isotropy is a measure a global measure of this directionality. Isotropy quantifies the directionality of the tubes and is defined as $\frac{\sum l \cos a}{\sum l \sin a}$ where l is the tube length and a is the tube angle. Tubes that are nearly aligned have a high isotropy and tubes that are randomly oriented have a low isotropy. Figure 4 shows the isotropy of a set of CNT networks with constrained tube angles. The tube density is 1.2 per micron and lengths are constant at 3 microns. The angles range from being constrained between -1 through $+1$ degrees to -90 through $+90$ degrees.

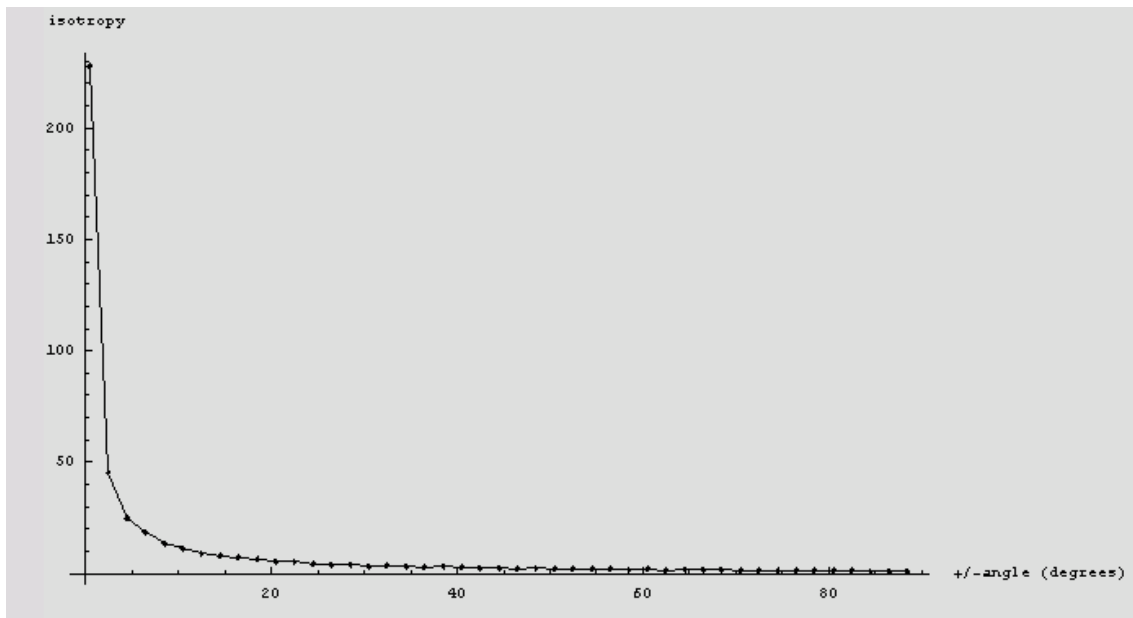


Figure 4 Isotropy decreases as tube angles assume wider ranges.

The angle of each tube can be considered as encoding information. Entropy, from an information theoretic viewpoint, measures the amount of information. Angle entropy is defined in this paper as $-\sum \text{Pr}(a) \log_2(\text{Pr}(a))$ where a is the tube angle and Pr is the probability of a tube of angle a given the network under analysis. The angle entropy of the network analyzed in Figure 4 is shown in Figure 5. Clearly, the more random the angle, the more angular entropy exists and thus there should be a relationship between isotropy, angular entropy, the type of networks that are formed, and ultimately, their performance and resilience to metallic tubes.

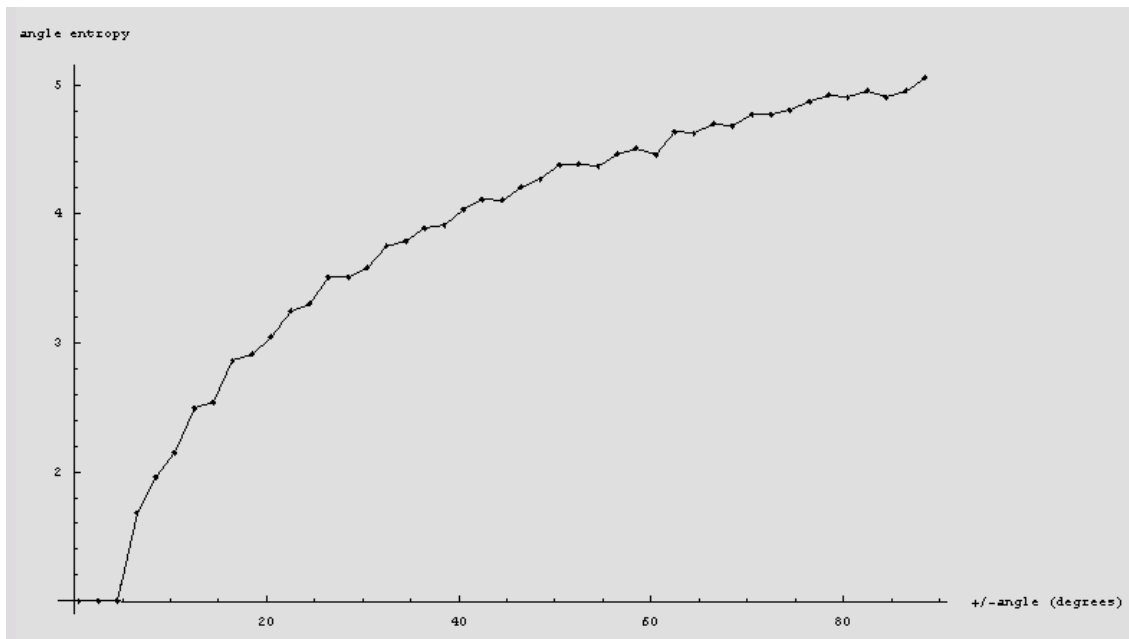


Figure 5 Angle entropy increases as the range of tube angles increases.

Clearly there is a relationship between isotropy and angle entropy as shown in Figure 6 for the same networks analyzed in the previous figure. High angle entropy implies that the directionality and thus the isotropy are low. Information can be stored in tube angles; reading the information from the change in resistance of tube angles is discussed in Ref 6.

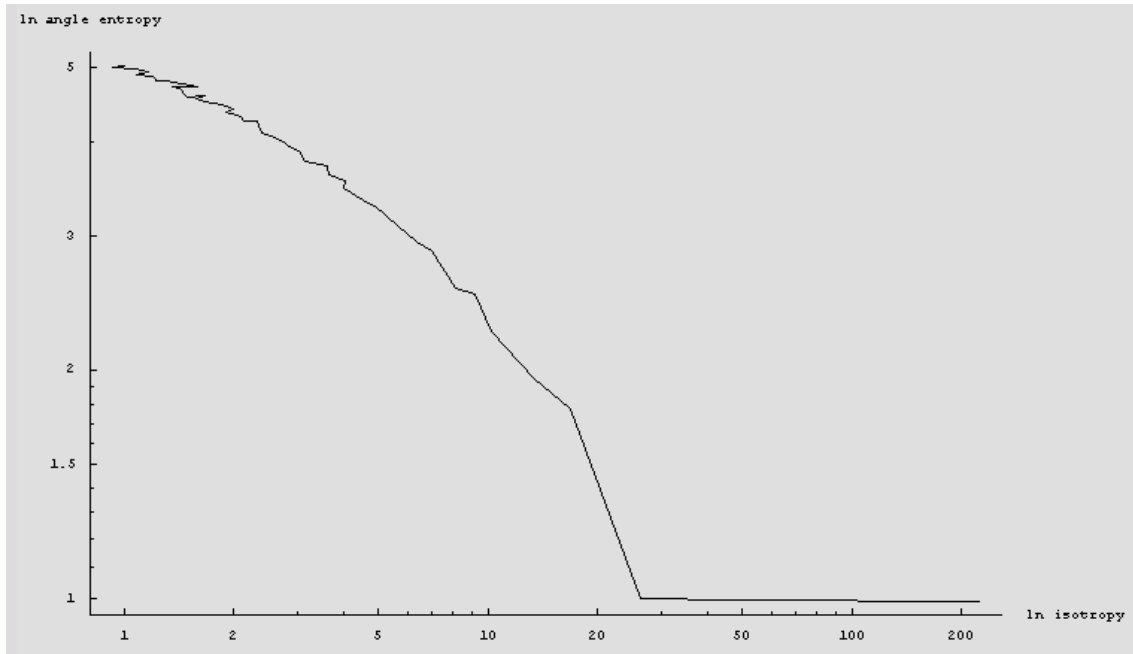


Figure 6 Natural Logarithm of angle entropy decreases as natural logarithm of isotropy increases.

As isotropy increases and entropy decreases, the density of tube intersections increases. Greater angular variation enables the tubes to intersect nearer to one another. The inter-tube contact resistance has a greater impact as intersection density increases. There is also an impact on the probability of percolation, which is considered in detail in a future paper by the same authors.

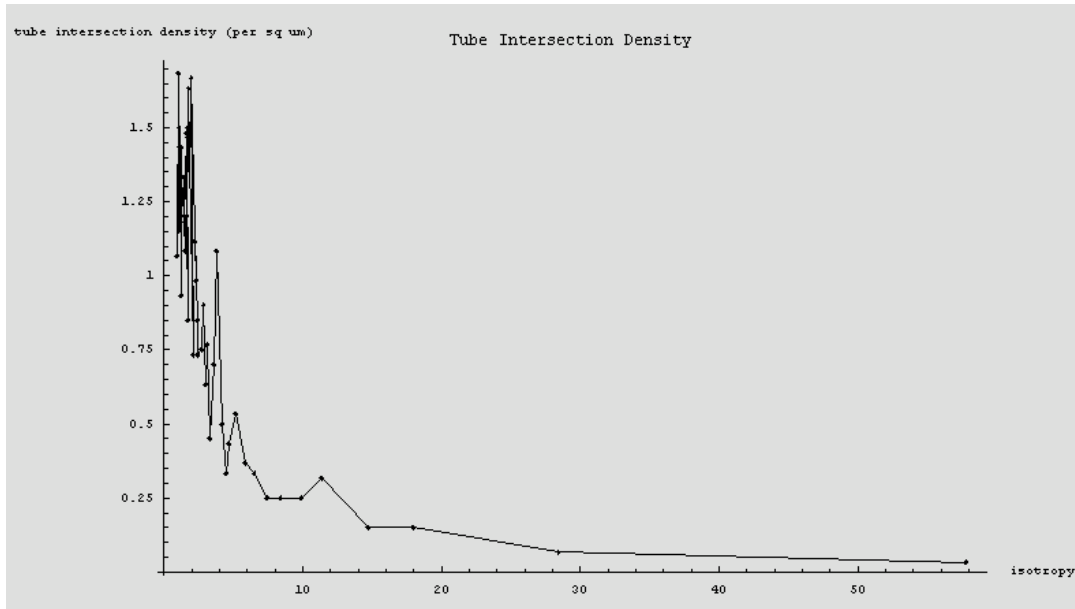


Figure 7 The density of tube intersections (nodes) varies inversely with isotropy.

Characteristics of CNT Networks

For any given orientation of nanotubes, the corresponding network $G(V, E)$ is extracted and resistances are assigned based upon the probability that a tube is either a pure carbon nanotube of 10^6 ohms when the gate is 'on' (10 volts) and 10^{12} ohms when the gate is 'off'. Impure (solid nanotubes) remain at 10^6 ohms regardless of gate voltage and the probability of a solid tube is 0.33.

The network formed by the overlapping nanotubes is extracted by determining the location of junctions. The gate area is overlaid on this network and virtual vertices are added as source and drain; the virtual vertices are assigned edges with no resistance to each nanotube that is adjacent to the source or drain edge of the layout respectively. The equivalent resistance of the network of resistors across the virtual source and drain is determined by (5) where l_i is the i^{th} eigenvalue of the graph Laplacian and $\varphi_{i\alpha}$ is the α component of the i^{th} eigenvector of the graph Laplacian⁴.

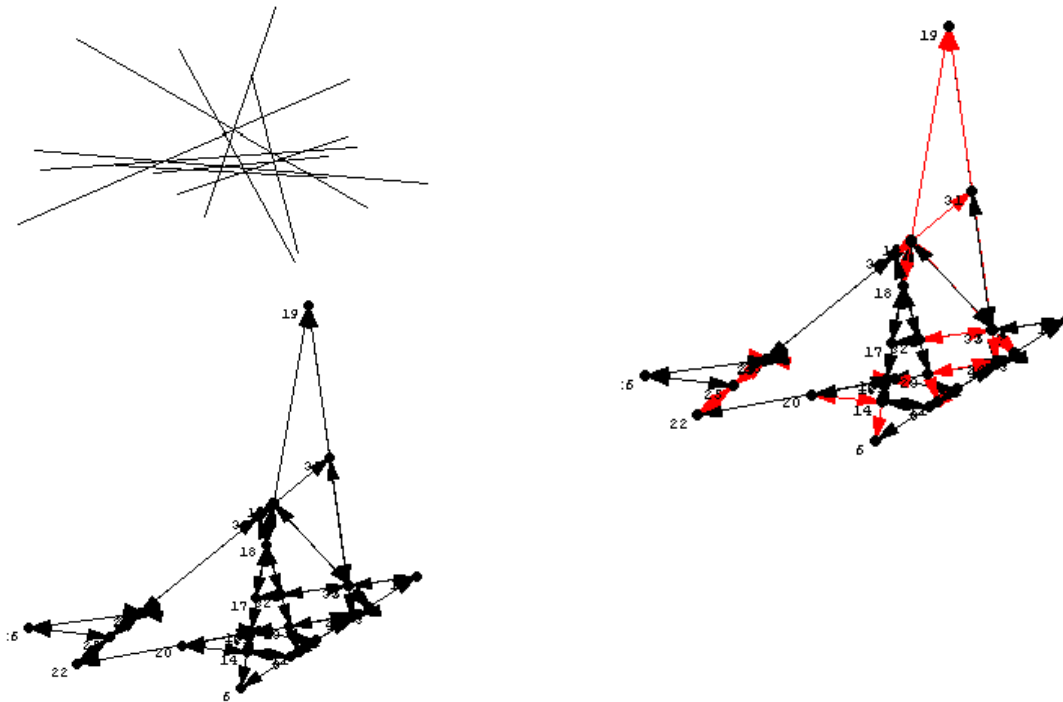
$$R_{sd} = \sum_1^N \frac{1}{l_i} |\varphi_{is} - \varphi_{id}|^2 \quad (5)$$

The graphs for large numbers of tube layouts with different distributions of locations, angles, and lengths have been generated. An example is shown in Table 1.

Table 1 Example of random CNT network generation: 10 tubes, angles uniformly distributed from 0 through π radians, tube centers are distributed in an area of 5 by 5 microns and tube lengths are randomly distributed from 5 to 20 microns, and the probability of a metallic edge is 0.33. The graph on the right highlights the metallic tubes (red).

```
g1 = CreateRNet[10, 0, 180, 5, 10, 5, 10, 5, 20, .33]
```

```
ShowLabeledGraph[g1]
```



Virtual source and drain locations are specified. This results in the addition of virtual nodes representing the source and drain as shown in Figure 8.

ShowLabeledGraph[g1]

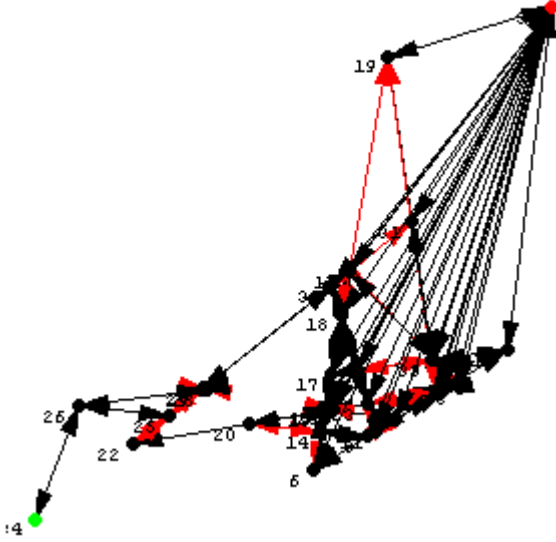


Figure 8 Virtual source and drain nodes added to the graph from Table 1.

Consider the relation in (1), namely, $f(t_{xy}, \theta, d_t) \longrightarrow G(V, E)$. Note that tube center locations t_{xy} and tube angles θ , are random variables. Tube density d_t is the number of tubes per unit area and is not considered a random variable in this analysis. Intuitively, one would expect the anisotropy (6), to have an impact on vertex density d_v .

$$\frac{\sum_{i=1}^N |\cos \theta_i|}{\sum_{i=1}^N |\sin \theta_i|} \tag{6}$$

In (6), the x component of each tube is $L_i \cos \theta_i$ and the y component of each tube is $L_i \sin \theta_i$ where L_i is the length of the i^{th} tube. If tube lengths are infinite, the number of vertices in $G(V, E)$ is defined as in (7). The intuition is that each new tube will overlap with $n-1$ existing tubes assuming no tubes are exactly parallel, yielding an additional $n-1$ nodes. Figure 9 shows the simulated number of the extracted graph nodes versus tubes

while Figure 10 shows a simulation versus the analysis. The simulation has a lower number of nodes because it assumes infinite tube lengths. The simulated nodes were finite; as the tube lengths increase, it is expected that the actual number of nodes would approach the analytical result.

$$|V| = n_t = \left(\sum_{i=1}^{t-1} t \right) \approx \frac{t^2}{2}, n_1 = 0, n_2 = 1 \quad (7)$$

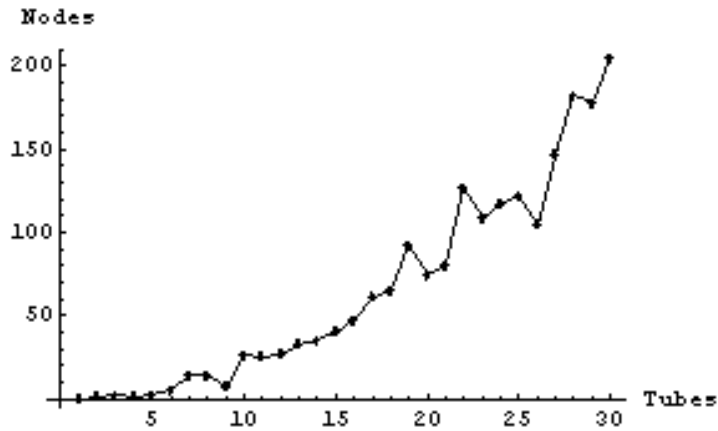


Figure 9 Nodes (tube intersections) versus total number of tubes. Tube angles are uniformly distributed from $-\frac{\pi}{4}$ to $\frac{\pi}{4}$ radians and tubes lengths vary uniformly from 3 to 10 microns in a 5 by 5 micron area.

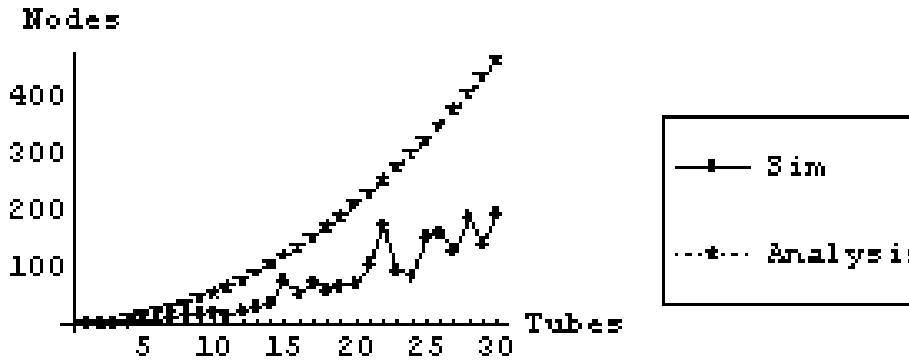


Figure 10 Simulated versus analytical results for tube angles uniformly distributed from 0 to $\frac{\pi}{2}$ radians. Analytical results assume overlaps from infinite tube lengths, thus the analytical results are an upper bound on the actual number of nodes.

Determining the number and density of vertices when tube lengths are finite becomes more complex. Equation (7) needs to be modified such that each term includes the probability of overlap between tube pairs as shown in (8), (9), and (10) where then probability of overlap is defined in terms of the probability of overlap in both the x and y components of tube pairs.

$$P_{ij}(o_2) = P_{ij}(o_x)P_{ij}(o_y) \quad (8)$$

$$P_{ij}(o_y | y, L, \theta) = P_{ij}(|y_i - y_j| < (L_i \sin \theta_i + L_j \sin \theta_j)) \quad (9)$$

$$P_{ij}(o_x | x, L, \theta) = P_{ij}(|x_i - x_j| < (L_i \cos \theta_i + L_j \cos \theta_j)) \quad (10)$$

Combining equations (8), (9), and (10) with (7) yields (11). The analysis from (11) is plotted versus actual in Figure 11.

$$|V| = P_{ij}(o_i) \binom{n}{2} \quad (11)$$

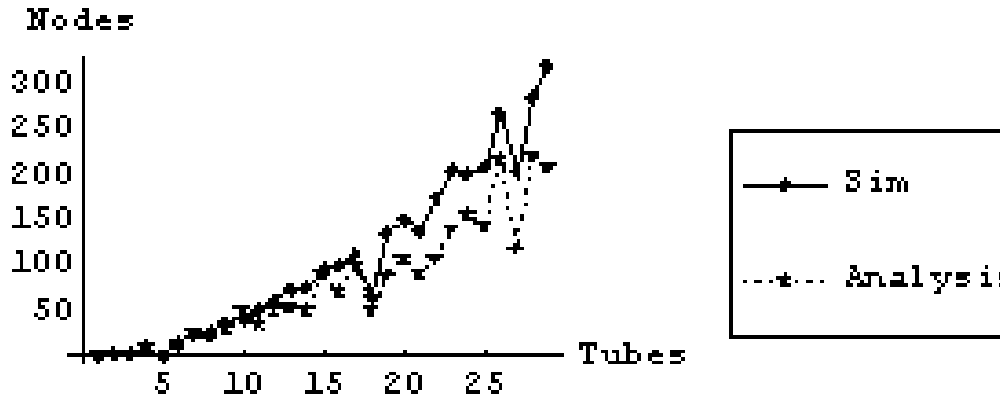


Figure 11 Probabilistic analyses versus simulation results using actual tube lengths.

A maximum number of vertices are generated when the difference between the x, y values are small, that is a high concentration of tubes, when L is large, and when θ is $(+/-)\pi/4$ radians or $(+/-)3\pi/4$ radians. The concentration of tubes required for a connected network across the gate increases at these angles. The relation between L and θ to create a connected network for a given concentration of tubes in area wL_{sd} also needs to be determined. If tube lengths are held constant and each tube center is located farther apart, then tube angles must be reduced in order to achieve a connected graph, which will reduce the number of vertices. Thus, there is an optimal range of θ for a given area that meets the requirement for a connected graph, but that also maximizes (or minimizes) the number of vertices in the CNT network $G(V, E)$. The probability of a connected network comes from (8). The requirement for a network reaching from source to drain is the probability that tubes i and j are connected and that i and j cover the

required distance. The expected distance covered that meets or exceeds the source to drain distance is shown in (12).

$$\sum_{i=1}^n \sum_{j=1, j \neq i}^n P_{ij}(o_2) \left(|x_i - x_j| + \left(\frac{L_i}{2} \cos \theta_i + \frac{L_j}{2} \cos \theta_j \right) \right) \geq L_{sd} \quad (12)$$

Data Transmission in a CNT network

Data transmission occurs via modulated current flow through the CNT network guided towards specific nano-destination addresses. The addresses identify spatially distinct areas of the CNT network. Since gate control is used to induce routes through the CNT network (discussed in detail next), nano-addresses are directly mapped to combinations of gates to be turned on that induce a path from a source to a destination. Figure 12 shows a conceptual view of the CNT network infrastructure. Note that in addition to gate routing control, sensors are often constructed directly from nanotubes in such a manner as to change the resistance based upon the amount and specificity of the material being sensed. Thus, the act of sensing may change the routing through the network.

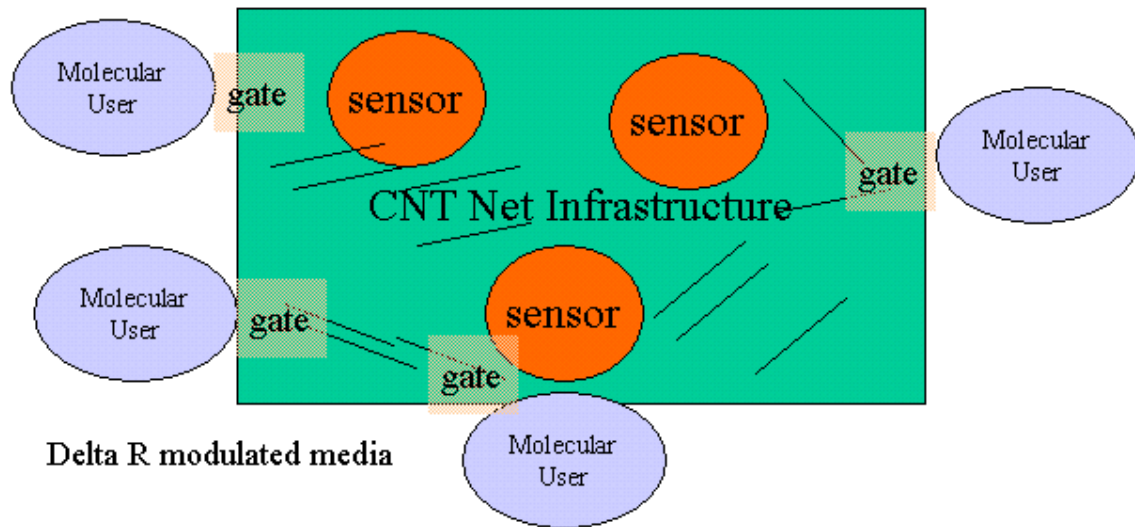


Figure 12 The CNT network infrastructure is comprised of resistance-modulated media routing information among molecular-level addresses.

Routing in a CNT Network

Given a CNT network, the mechanism used to route data through such a network must be considered. Consider a random CNT network with a matrix of gates as shown in Figure 13. When a gate is turned on, the nanotubes within the gate area become conducting. Properly choosing gates to turn on also changes the current flow to the edges of the CNT network, effectively creating a controlled network, which may act as a communications network or as weights in a neural network.

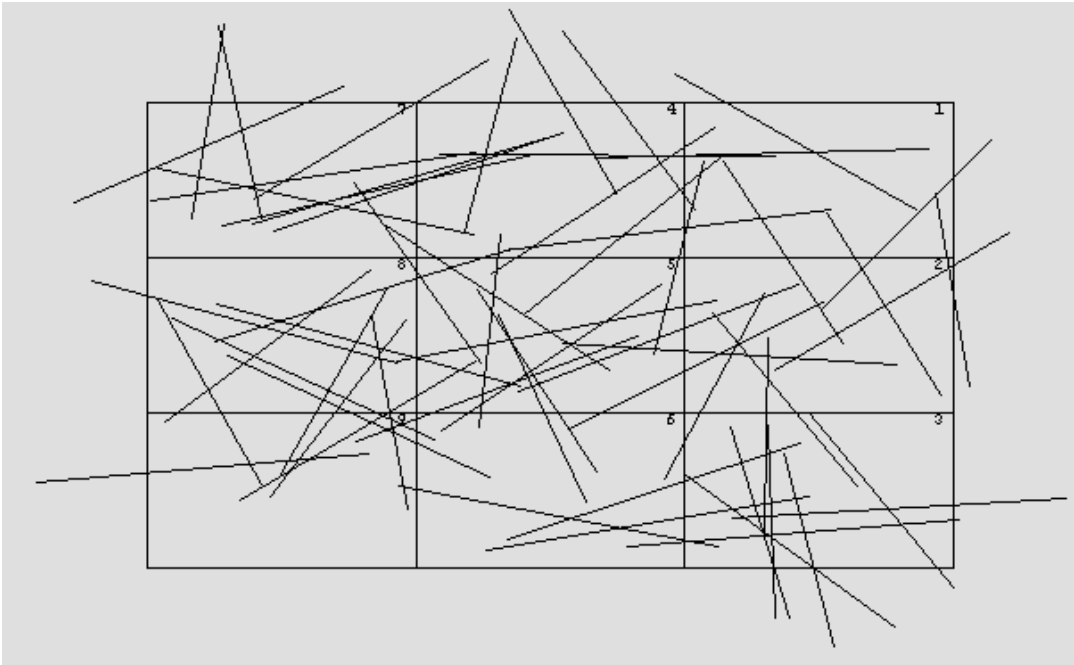


Figure 13 Above are a matrix of gates superimposed on a random CNT network. The gates are identified by number and when turned on, change the resistance of the semiconducting nanotubes within its area. Most nanotube sensing devices operate by changing tube resistance. A gate that is turned on, for any reason, may be used to route data through the network. Thus, the sensing elements, which sense by variation in resistance, may act simultaneously as routing elements.

The potential for such routing capability is simulated using a specific CNT network shown in Figure 14. The tubes shown in red are considered the outputs of this switch. Tube 52 is considered the input. The hypothesis is that in this anisotropic media, tubes are randomly dispersed at all possible angles providing an approximately equal propagation of current in all directions. Activating gates appropriately serve to channel the flow into desired directions.

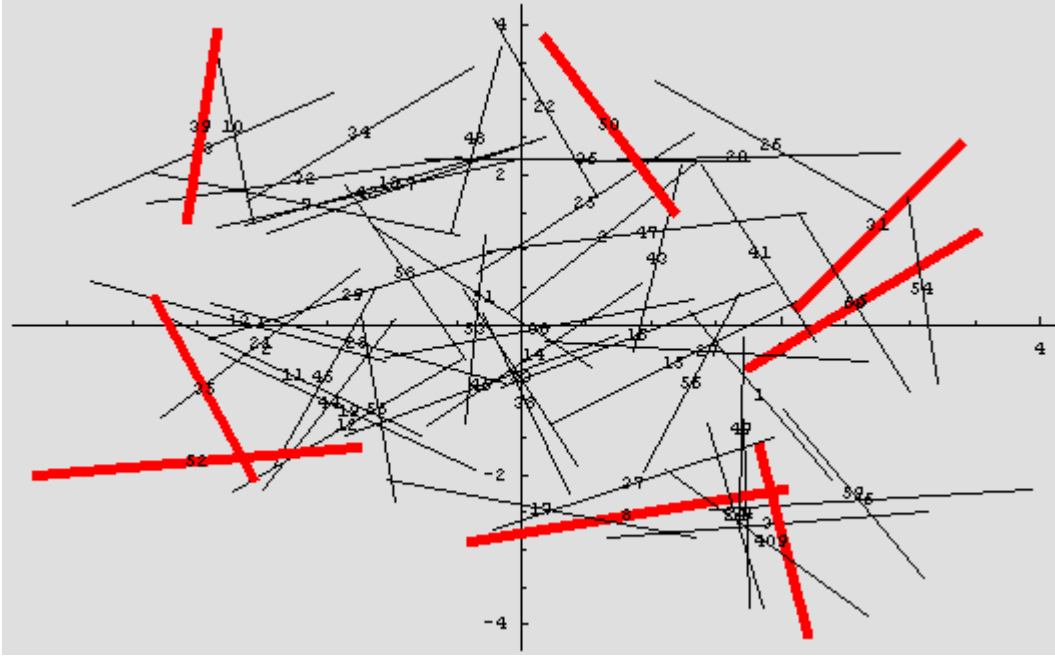
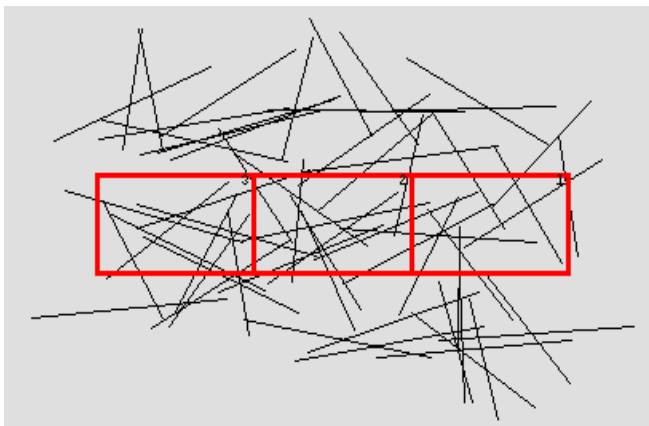
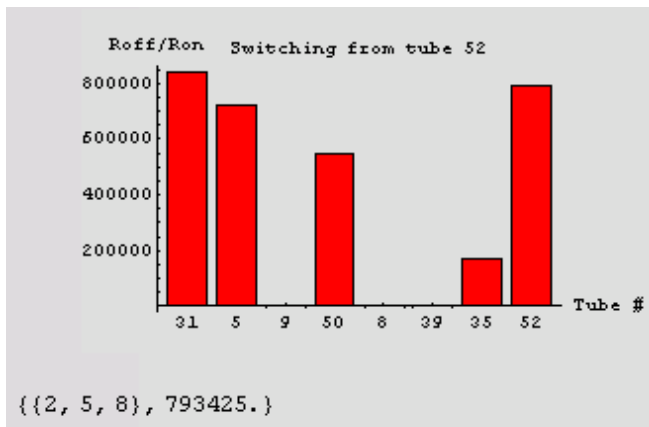


Figure 14 Tubes used for I/O when the CNT network is used as a communication network are shown in red. The red tubes correspond to I/O contacts, one for each area surrounding the network (areas shown in previous figure).

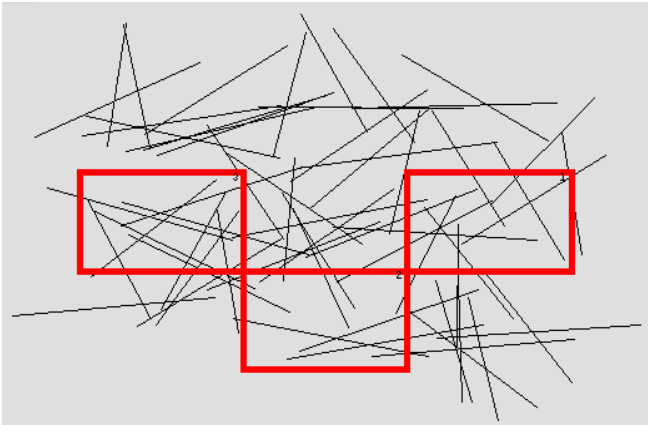
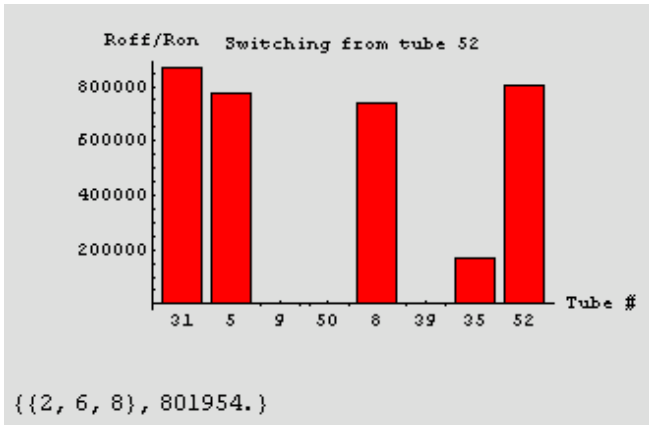
Using a relatively small 3×3 gate matrix, consider all $\binom{9}{3}$ possible combinations of gates turned on and the impact on the predefined output tubes. The ratio of the resistances from tube 52 to all output tubes when no gates are turned on R_{off} , to the resistance between same tube pair when combinations of the gates are turned on R_{on} is plotted on bar charts as shown in Table 2. The effectiveness of the routing capability is measured by the difference between the resistance ratio at each output and the expected resistance ratio at all outputs (13); only the most effective gate combination is shown for each output.

$$\max_{\text{ongates}} \left[\left(R_{off} / R_{on} \right)_{t \text{ arg etOutput}} - E_{\text{outputs}} \left[R_{off} / R_{on} \right] \right] \quad (13)$$

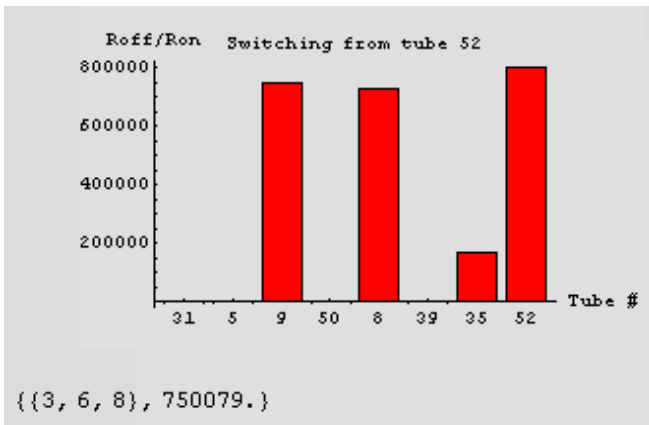
Table 2 The ratio of resistance with no gates turned on to the resistance with the indicated gates turned on is shown in the bar graphs for selected I/O tubes. The gates turned on that generate the bar chart values are shown beneath each chart. Tube 52 is the input tube for this example. The last number in the list below each bar graph is the resistance threshold distinguishing the output resistance ratio from the next highest ratio.



Resistance ratio and gate configuration for output tube 31.

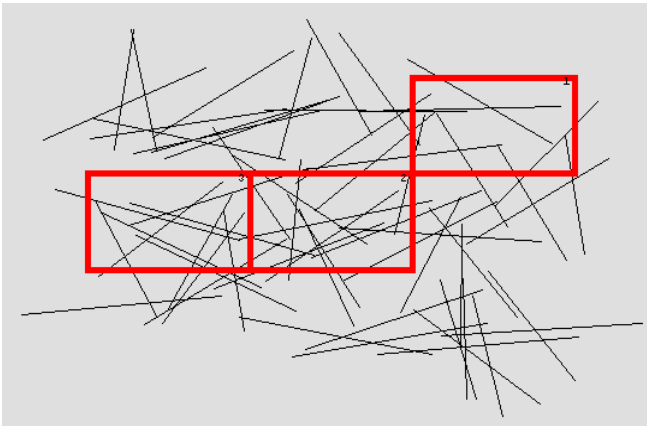
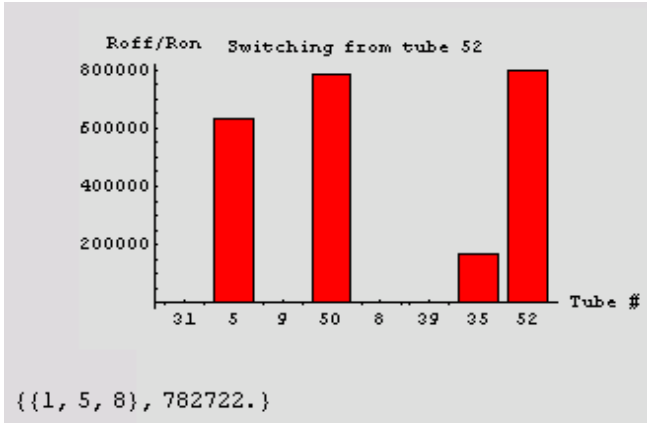


Resistance ratio and gate configuration for output tube 5.

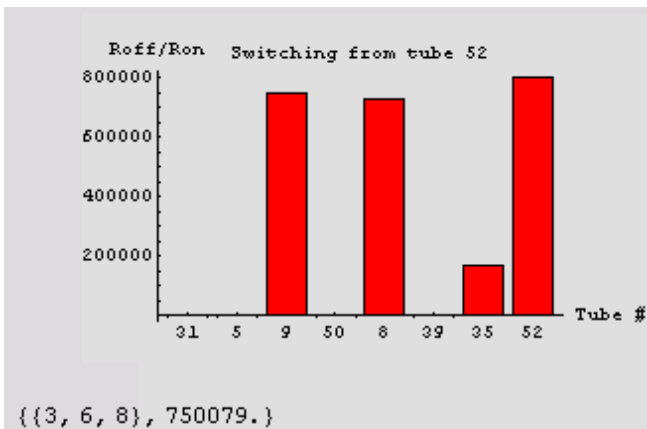


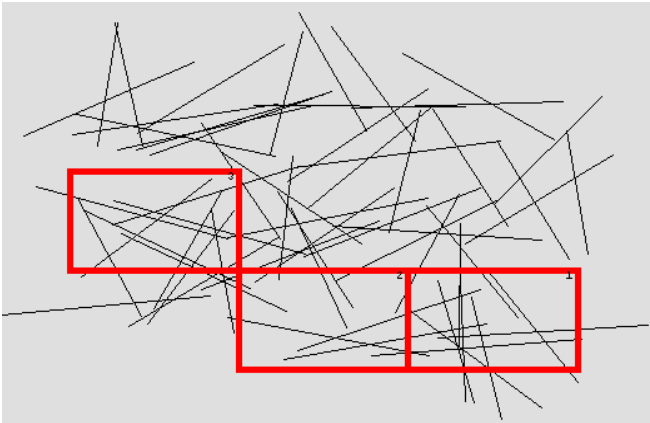
Resistance ratio and gate configuration for

output tube 9.

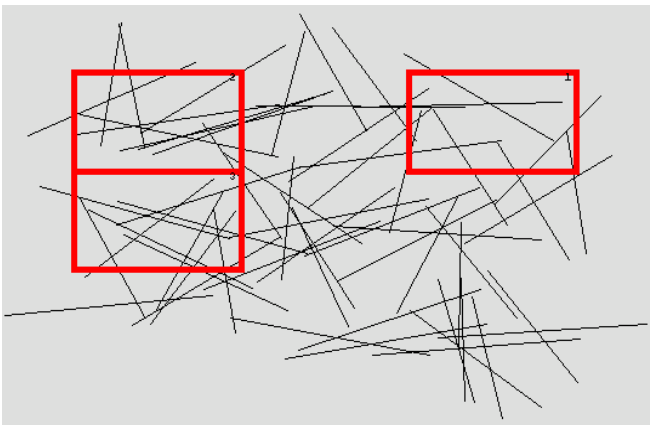
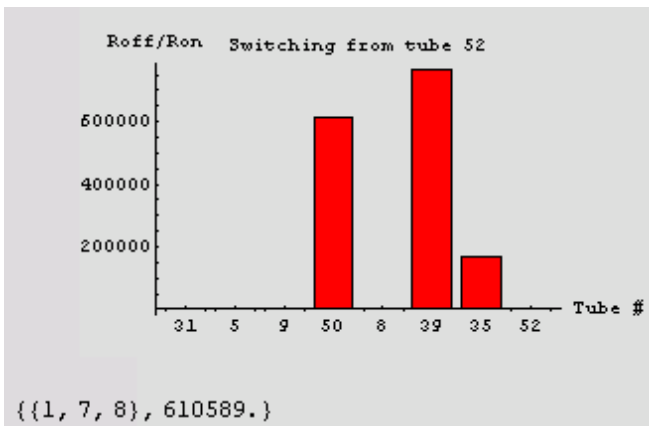


Resistance ratio and gate configuration for output tube 50.



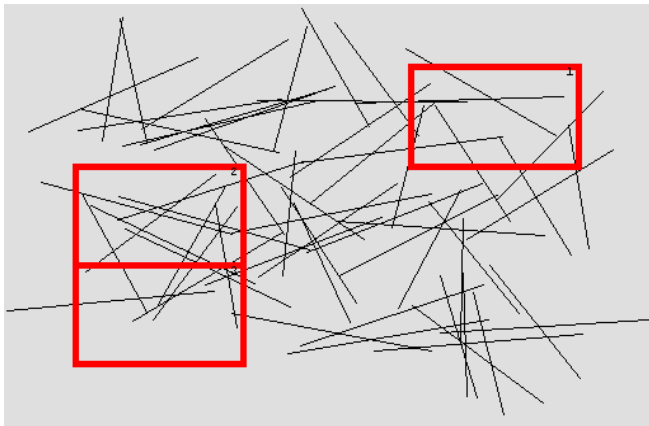
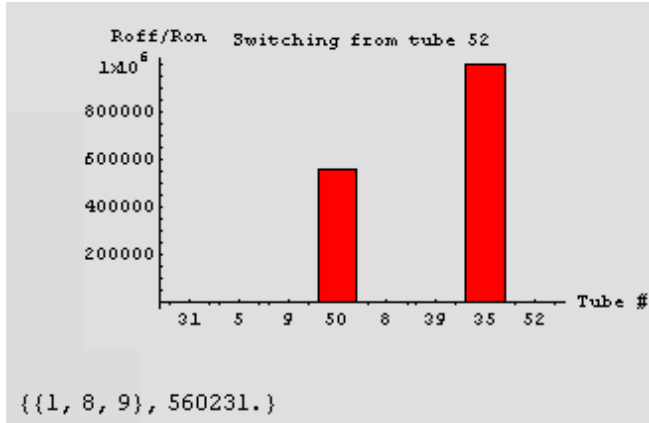


Resistance ratio and gate configuration for output tube 8.



Resistance ratio and gate configuration for

output tube 39.



Resistance ratio and gate configuration for output tube 35.

Conclusion

Information flow through a CNT network may be controlled in spite of the random nature of tube alignment. The same technique used for sensing in CNT networks, namely, change in resistance of semiconducting material, may be used to effectively route information. The traditional networking protocol stack is inverted in this approach because, rather than the network layer being logically positioned above the physical and link layers, the CNT network and routing of information is an integral part of the physical

layer. The potential benefits of better utilizing individual nanotubes within random carbon nanotube networks (CNT) to carry information is distinct from traditional, potentially less efficient and wasteful, approaches of using CNT networks to construct transistors which are then used to implement communication networks. In closing, the author would like to pose a theoretical question with significant practical impact, namely, whether one might achieve an information rate through the CNT network that approaches the maximum flow through the equivalent network graph, in other words, network coding at the level of individual nanotubes⁵.

References

1. Wolfram, S. *The Mathematica Book*, Fifth Edition, Wolfram Media, ISBN 1-57955-022-3, 2003.
2. Wolf, E. L. *Nanophysics and Nanotechnology*. ISBN 3-527-40407-4, Wiley-VCH, 2004.
3. Gupta, P. and Kumar, P.R. "Capacity of wireless networks," Technical report, University of Illinois, Urbana-Champaign, 1999.
4. Bush, Stephen F. and Li, Yun, "Network Characteristics of Carbon Nanotubes: A Graph Eigenspectrum Approach and Tool Using Mathematica," GRC Technical Report in press.
5. Kramer, Gerhard and Savari, Serap A., "Edge-Cut Bounds On Network Coding Rates," *JOURNAL OF NETWORK AND SYSTEMS MANAGEMENT*, Vol. 14, No. 1, March 2006, Special Issue On Management Of Active And Programmable Networks, Guest Editors: Stephen Bush And Shivkumar Kalyanaraman.

6. Bush, Stephen F. and Li, Yun, “Network Characteristics of Carbon Nanotubes: The Impact of a Metallic Nanotube on a CNT Network,” GRC Technical Report in press.

Correspondence and requests for materials should be addressed to S.F.B. (bushsf@research.ge.com).